Chapter 2

Principles of LCD Illumination Systems

As the expansion of TFT color LCDs, the LCD illumination systems of light weight, thin design, high luminance, and lower power consumption are required for more appealing applications. Conventionally, LCD illumination systems, i.e. LCD backlights, are composed of light source (Cold Cathode Fluorescent Lamp (CCFL) or Light Emitted Diode (LEDs)), reflector, lightguide, prism sheets, and diffuser sheets. In this chapter, we describe the principles of key components in LCD illumination embodiment. First, the working principle and the design of lightguide plate, shape and optical patterns, are discussed. Followed by characterizing the function of optical films, such as prism sheets, diffuser sheets, and polarizing sheets. Then, some concerned issues while designing the backlight systems are studied. Additionally, the simulated procedures are introduced to confirm that the proposed designs can meet the required properties of LCD illumination systems. Finally, a briefly summary will be given.

2.1 Working Principle of Lightguide Plate

For pursuing higher brightness, uniformity, and adequate light efficiency, lightguide always plays the key components in the LCD backlights. As a result, various designs and applications of lightguides were reported and developed. Nevertheless, before revealing the contents of proposed novel illumination systems, the fundamental principle of lightguide shall be clearly clarified. Lightguide is conventionally made of plastic substrates, such as Polymethyl methacrylate (PMMA) or Polycarbonate (PC). Because the refractive index of PMMA/PC is significantly

larger than the refractive index of air, the total internal reflection occurs while the incident angles larger than the critical angle θ_c.

$$\theta_c=\mathrm{Sin}^{-1}(1/n) \qquad (2\text{-}1)$$

where n is the refractive index of lightguide. For example, the refractive index of PMMA is approximately 1.49. Thus, the critical angle of PMMA substrate equals to 42.2°. As shown in Fig. 2-1, if the incident light from the light source is coupled into the lightguide at large angle θ_1 of approximate 90°, light is refracted at θ_2 of 42.2°. Then, light incidents on the air/PMMA interface at 47.8°, which is significantly larger than the critical angle 42.2°. Therefore, total internal reflection of light occurs. Hence, light is trapped in the lightguide.

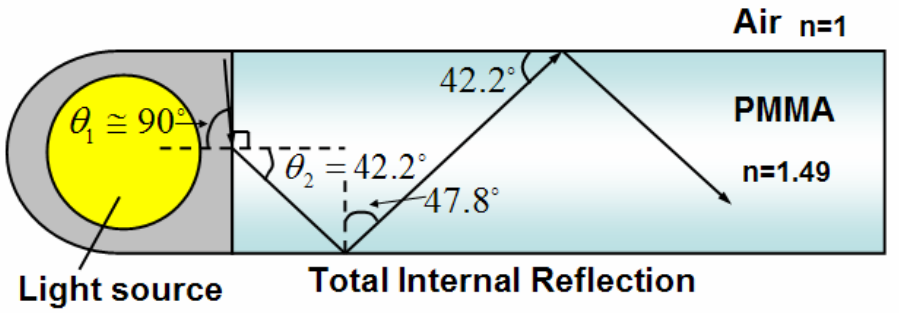

Fig. 2-1. Total internal reflection of incident light in the lightguide with PMMA substrate.

Dots patterns or micro-structures are fabricated on the back side of lightguide to scatter incident light; thereby extracting trapped light. As a result, total internal reflection can be destroyed. Conventionally, white ink composed of high reflection materials, such as TiO_2 and $BaSO_4$, is printed on the back side of lightguide to form the dots patterns. Reflective white ink is not covered the entire area of the back side of the lightguide.[1] In contrast, dots patterns are distributed in gradience. In the region closer to the light source, the dots patterns can be either smaller in the size or sparser

in the distribution. Contrarily, the dots patterns are either larger in the size or denser in the distribution in the region far away the light source. Additionally, the distribution of the dots patterns change with the configurations of light sources as well. In the following sections, we will detailedly discuss the design and optical patterns of lightguides by classifying the configuration of light sources, types of lightguide, and shapes of micro-structures.

2.1.1 Optical Design of the Lightguide by the Configuration of Light Sources

By the classification of the configuration of light sources, lightguides can be concluded into single and dual edge-lighted types.

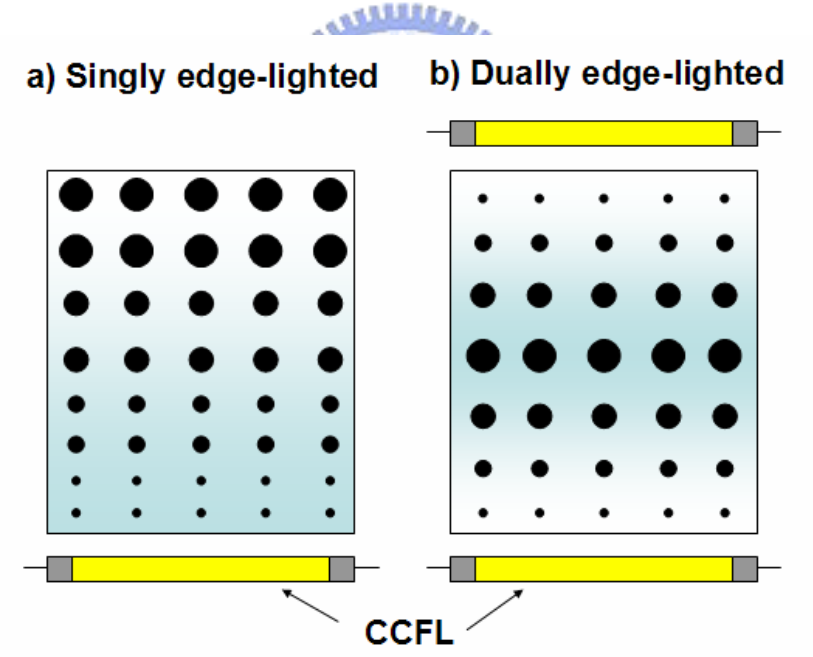

Fig. 2-2. Schematics of (a) single edge-lighted and (b) dual edge-lighted lightguides.

Fig. 2-2 demonstrates single and dual edge-lighted lightguides, respectively. For single edge-lighted lightguides, the dots patterns are distributed in gradience from one side to the other side. In contrast, for dual edge-lighted lightguides, the dots patterns

are centrally dense-distributed.

2.1.2 Optical Design of Lightguide by Type of Lightguides

For single edge-lighted lightguide, the shape of lightguide is conventionally a rectangular plate. Therefore, light remains totally internal reflected until light is scattered by the dots patterns. However, portion of light is absorbed by the material of pigments, TiO_2. Additionally, large amount of light is directly extracted at the end surface of lightguide, thus, resulting in serious energy loss. Though, a reflector, which is the so-called end reflector, can be placed at the end surface of lightguide to reduce the energy loss. Nevertheless, inadequate light utilization efficiency is unavoidable. Many approaches were reported to further improve light utilization efficiency. A wedged lightguide is one of the examples that can effectively enhance light utilization efficiency. As shown in Fig. 2-3, the back plane of lightguide is designed to be inclined at a tiny angle (around 1°~2°) with respect to the horizon. When T.I.R of light occurs in the wedged lightguide, the incident angle of light is decreased by the inclined angle of lightguide after every bounce on the inclined back plane. As a result, after several bounces of T.I.R, light is extracted from the lightguide because the incident angle becomes smaller than the critical angle. Generally, a wedged type of lightguide can increase the light utilization efficiency by a factor of 20% compared with a rectangular lightguide. As a result, a wedged type of lightguide becomes the major trend of the lightguide designs.

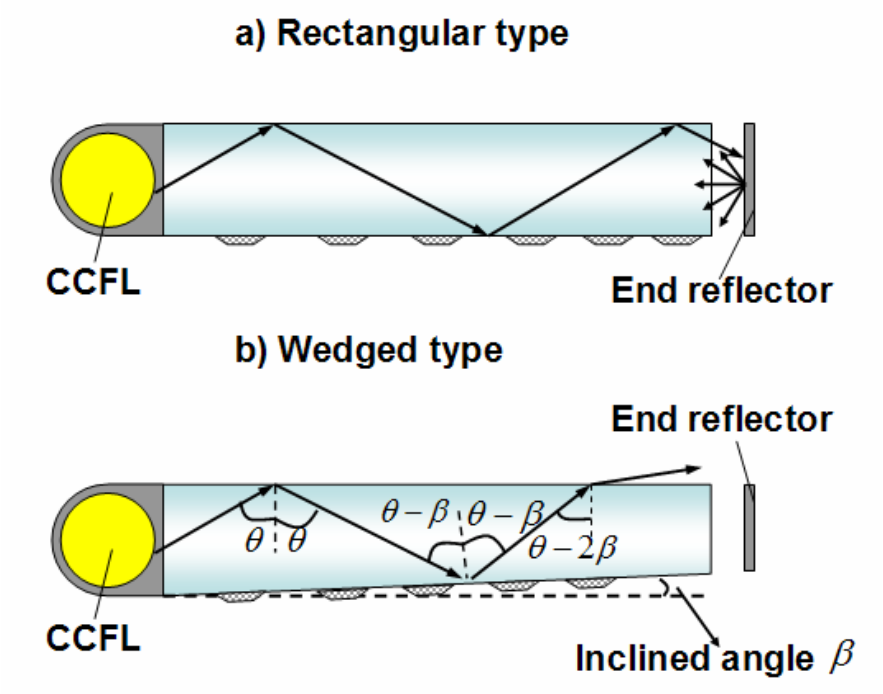

Fig. 2-3. Schematics of (a) rectangular type and (b) wedged type lightguides

2.1.3 Optical Design of Lightguide by Shapes of Micro-structures

For printed lightguides, the incident light is scattered by the reflective dot patterns on the back side of lightguide. Conventionally, the diameter of the dots varies from 0.25 to 1.2 mm, according to its position. These dots scattered the trapped light inside the lightguide. Nevertheless, the scattering of light leads to an energy loss of light. Additionally, a wavelength dispersion accompanying with color degradation over the backlight occurs. In order to utilize the light more efficiently, a modification of the lightguide is indispensable in the backlight unit. As a result, various lightguides are proposed to further enhance light efficiency and brightness of the backlights by using different shapes of micro-structures, such as micro reflector (MR), micro grooves, and micro pyramids. Various micro-structures are made on a metal mold, then, transferred to an acrylic material on forming, which is the so-called injection molding process. This fabrication can resolve the issues due to scattering process. Simultaneously, time and cost are less demanded in fabrication compared with screen

printing approach. In order to reveal the functioning of the devices, we will describe the principle and designs of various micro-structures in the following section.

(I) Micro-reflector (MR)

In the year of 1999, K. Kalantar proposed a novel backlight composed of an array of circular plano-convex optical micro reflectors (MR), which is designed and molded on the back side of the lightguide instead of white scattering dots.[2] An arbitrary direction of emanating light on the surface of lightguide can be designed by forming the MR element. The small size of MR element made it possible to have smooth surface, high reflection and no more scattering light, thus, reducing loss of energy. Generally, the diameter and height of MR is about 100±2 μm and 10±1 μm, respectively. These reflectors can be used to control the direction of the reflected light shown in Fig. 2-4.

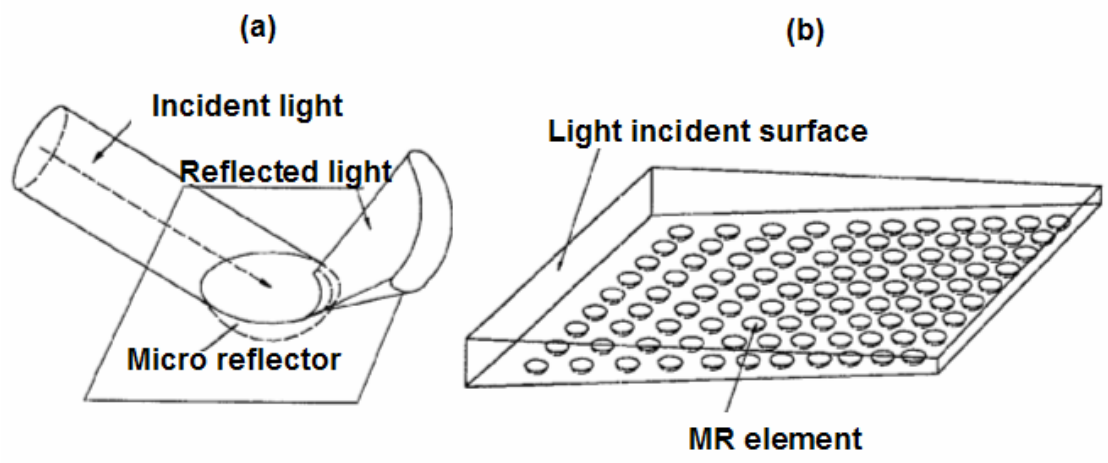

Fig. 2-4. Schematics of the micro-reflector array. (a) Incident light on the optical surface of the MR element is reflected. (b) Array of the MR elements on the bottom surface of the lightguide.

As the rules of designs of dot patterns, MR elements are distributed in gradient for

obtaining high uniformity of luminance. The direction of reflected light can be determined by ratio of the depth to the diameter of MR element. As a result, extracted and trapped portion of light can be controlled to achieve better uniformity in the entire backlight. Furthermore, a smooth optical surface effectively reduces the energy loss due to scattering process. Hence, using this type of lightguide, luminance can be increased by 3%~20%.[3]

(II) Micro-grooves

Micro-grooves are another popular type of lightguides instead of printed lightguides. The easy fabrication by slot cutting method makes this design more appealing. As shown in Fig. 2-5, mirror surfaces of micro-grooves avoid the occurrence of T.I.R of light, so that light can be extracted from the lightguide.

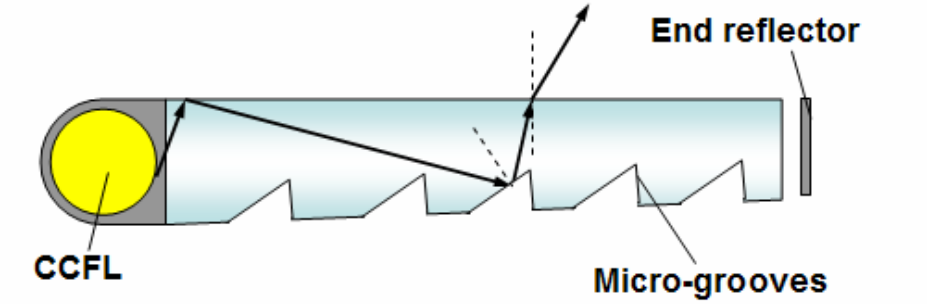

Fig. 2-5. Schematics of lightguide with micro-grooves on the bottom surface.

By tuning the pitch, width, and depth of micro-grooves, light distribution on the outcoupled plane of lightguide can be modulated. Generally, the pitch is ranging from 400 to 800 μm. The width and depth of micro-grooves are 30~200 μm and 15~100 μm, respectively.[3] Micro-grooves are advantageous in luminous intensity enhancement because the smaller scattering angular distribution is obtained, thus, resulting in enhancement of normal luminous intensity. Compared with screen

printing approach, luminous intensity can be increased by 10%. Nevertheless, the issues of moiré patterns usually occur in this type of lightguides. The superposed periodic structures of lightguide and prism sheets arouse the moiré patterns, thus, resulting the uncomfortable feeling while viewing. Hence, either applying a diffuser or rotating prism sheets by a tiny angle is the most conventional way to suppress the moiré.

(III) Micro-pyramids

For the lightguide with micro-grooves, mirror surfaces of micro-grooves destroy T.I.R of light, so that light can be extracted from the lightguide. However, micro-grooves are conventionally distributed in one direction. Light can be collected and hence enhanced in luminous intensity only in one direction, yet, light is no longer collected in the orthogonal direction. In order to improve this issue, a lightguide with micro-pyramids was therefore developed, which is demonstrated in Fig. 2-6.

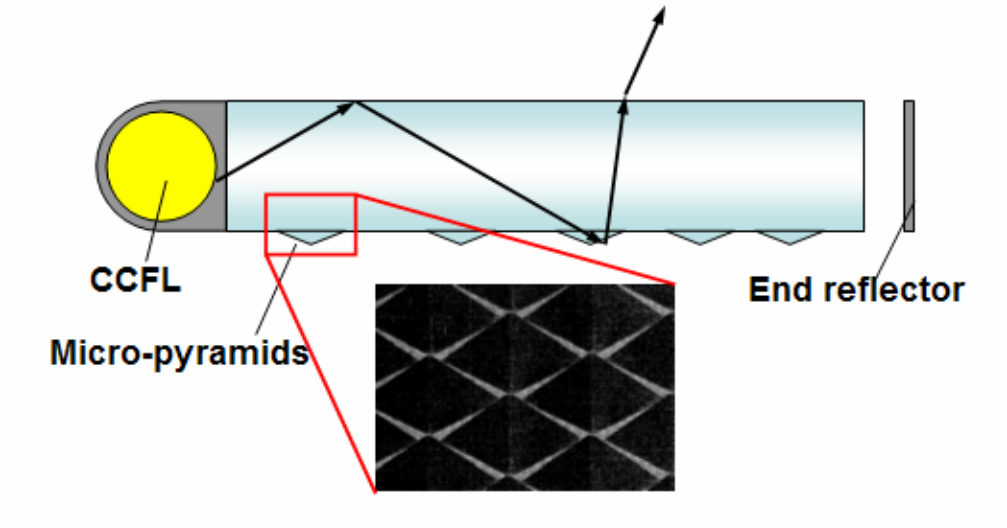

Fig. 2-6. Schematics of lightguide with micro-pyramids on the bottom surface.

Micro-pyramids are defined on the metal mold by two-dimensional diamond

machining. The patterned mold is then used in injection molding or hot embossing process to duplicate the micro-pyramids on acrylic substrate. The angle of micro-pyramids is around 100˚.[4] However, the angles of micro-pyramids in two respect directions may also have different values aiming for various divergent angles of backlight. Generally, the luminous intensity can be enhanced by 20% compared with printed dot pattern approach.

2.2 Brightness Enhancement Film (BEF)

Because the emitted direction from the lightguides is not concentrated on the normal viewing direction, the demand of brightness is not satisfied for LCD illuminations. In order to modify the direction, thus, collecting light toward the desired direction, prism sheets were developed as a key component for modification of angles. The 3M company has developed the prism sheets, which is so-called Brightness Enhancement Film (BEF). The Brightness Enhancement Film (BEF) is a ridged transparent plate, with a cross-section as shown in Fig. 2-7.

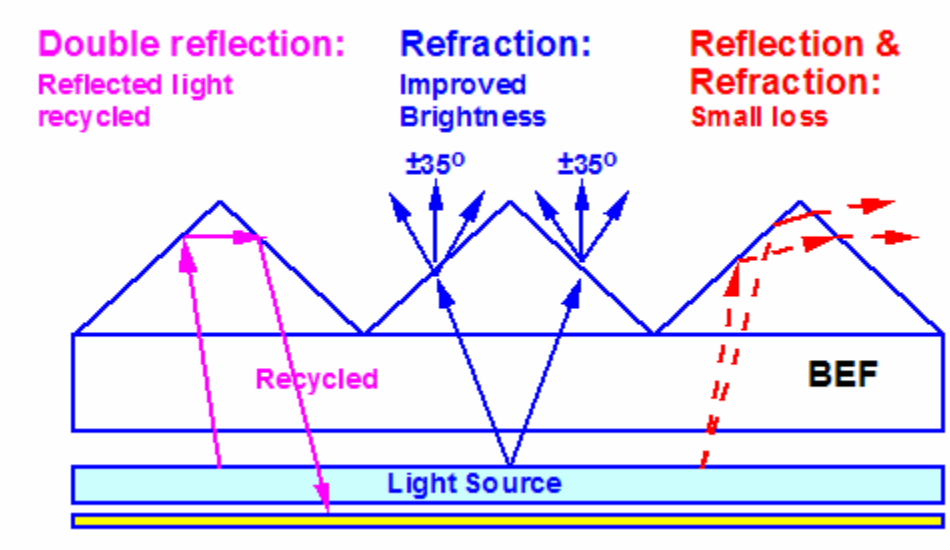

Fig. 2-7. The operation of Brightness Enhancement Film (BEF).

The changes in refractive indices at the solid-air interface causes refractions and

reflections. For the incidence angle larger than the critical angle at the interface of prisms, light is hence T.I.R. The reflected light is then recycled by a reflective sheet, which is placed beneath the lightguide plate. Besides, refraction of light results in a confined emitted cone toward the normal viewing. Most widely used BEF is BEFII 90/50, which the vertex angle and pitch of prism are 90° and 50 μm, respectively. As indicated in Fig. 2-7, most extracted light from the backlight is concentrated within ±35° with respect to the normal direction.[5] By using one BEF in the conventional lightguides, luminous intensity in the normal viewing can be increased by a factor of 1.58. Additionally, using two crossed BEFs, luminous intensity in the normal viewing can be further enhanced by a factor of 2.14.

Although BEF can greatly enhance luminous intensity in the normal viewing, additional cost and thickness usually hinder its applications. In order to avoid the bending of prism sheets, thickness larger than 400μm is essential. The additional thickness is against the trend of thin and light backlights. This issue becomes more conspicuous especially in mobile applications. Therefore, a novel lightguide with patterned micro-structures on both the back and the top sides was proposed, as shown in Fig. 2-8.[6] On the back side of lightguide, dots patterns or micro-structures are covered. Additionally, on the top side of lightguide, micro-grooves are patterned to replace the original BEF. Even for using two crossed BEFs in the lightguide, one sheet of BEF can be left out to further reduce the cost and thickness of the backlight module.[6] The backlight is therefore becoming more compact.

Recently, collimated lightguides were developed aiming for enhanced luminous intensity in the normal viewing without using any prism sheets. The prism array on the back side of lightguide is utilized to concentrate the emitted cones of light within ±20° with respect to the normal direction. The most famous one is Omron's prism-sheetless backlights.[7] As a result, the prism sheets can be left out.

Nevertheless, the trade-off is the narrow viewing angle, which constrains the collimated backlights in the small sized applications.

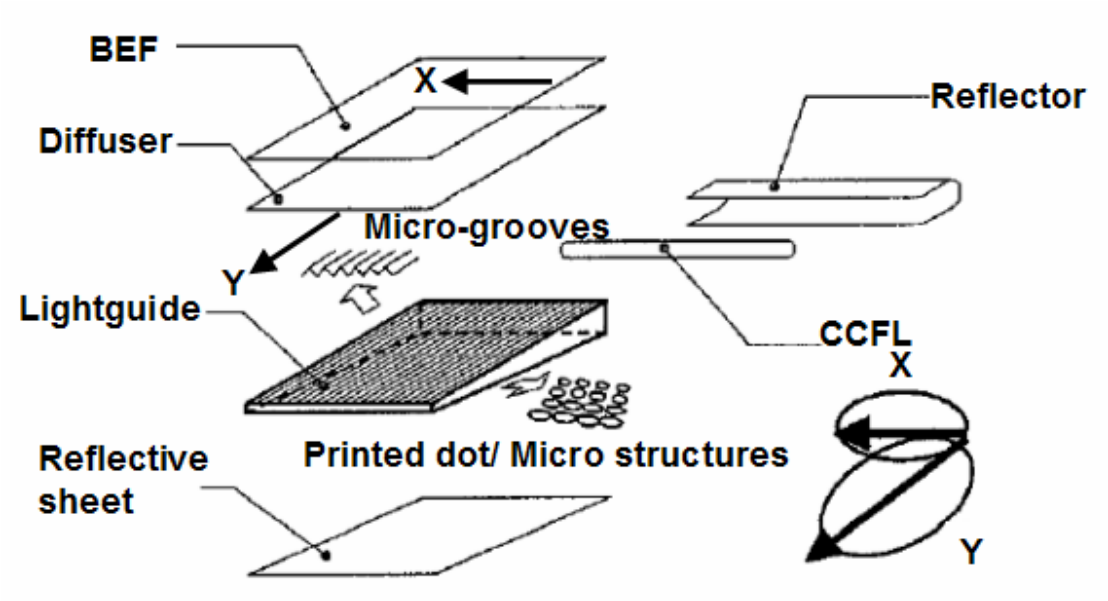

Fig. 2-8. Schematics of lightguide with dual patterned surfaces. On the bottom surface, printed dots/ micro structures are covered. On the top surface, micro-grooves are line in Y direction. Only one sheet of BEF, which is line in X direction, is needed.

2.3 Diffuser Films

Diffuser films are widely used in commercial backlight products to make light distribution more uniform. There are two kinds of diffuser films, the conventional diffuser film and the protective diffuser film, which have almost the same structure as shown in Fig. 2-9. The diffusive layer on the top of the base film has some beads buried in a binder layer and other beads protrude partially out of the binder layer. A non-stick layer on the back of the base film has beads buried separately and protruding partially out of the binder layer. Generally, the diffuser film is located on the top of the lightguide, but the protective diffuser film is placed on the top of the upper BEF. The functions of the former are to enhance the homogeneity of light by diffusing light and to enhance the luminance by changing the light output to the

appropriate direction for the BEF. On the other hand, the latter are to minimize the degree of damage to the BEF, to cut down the glare due to the BEF and to enhance the viewing angle.[8]

In addition, diffuser films provide the function of enhancing the image quality of the display. Except the suppression of moiré patterns, diffuser films can also avoid the specular reflection of light. Due to reflection of light by the mirror surfaces of micro structures, the image on the display is somehow blurred. Furthermore, non-uniformity of luminance easily arose at the edge of LED backlights because of confined emitted cones of LEDs. Therefore, diffuser films become urgent for further improving uniformity and suppressing moiré and specular reflection.

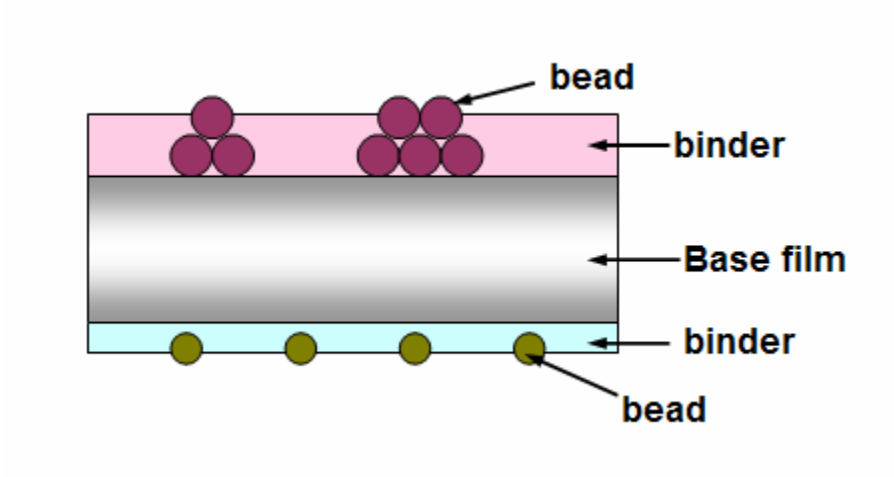

Fig. 2-9. The structure of diffuser film.

2.4 Polarized Light Propagation in Birefringent Media

LC doesn’t emit light by itself but modulates the transmission of light by rotating the polarization of light. Furthermore, polarization recycling is the main target to be achieved in LCD backlights. Therefore, basic physical background of polarization optics becomes essential for clarifying the operation principle of polarizing components and is introduced in the following sections. The polarization of

light wave is specified by the electric field vector **E(r,t)** at a fixed point in space, **r**, at time **t**. In the complex form representation, the electric field vector of a plane wave in the z direction can be given by

$$\mathbf{E}(z,t)=\mathrm{Re}[\mathbf{A}e^{i(\omega t-kz)}] \tag{2-2}$$

where **A** is a complex vector that lies in the xy plane. In consideration of the nature of curve which the end point of the electric field vector **E** describes at a typical point in space, the curve is the time-evolution locus of the points whose coordinates (E_x, E_y) are

$$\boldsymbol{E_x}=\boldsymbol{A_x}\cos(\omega t-kz+\delta_x), \tag{2-3}$$

$$\boldsymbol{E_y}=\boldsymbol{A_y}\cos(\omega t-kz+\delta_y), \tag{2-4}$$

where the complex vector **A** is defined as

$$A=\hat{x}A_x e^{i\delta_x}+\hat{y}A_y e^{i\delta_y}, \tag{2-5}$$

where A_x and A_y are positive numbers, $\hat{x}$ and $\hat{y}$ are unit vectors. By eliminating the term ωt-kz in the equation (2-5), we obtain

$$(\frac{E_x}{A_x})^2+(\frac{E_y}{A_y})^2-2\frac{\cos\delta}{A_xA_y}E_xE_y=\sin^2\delta, \tag{2-6}$$

where $\delta=\delta_y-\delta_x$. All the phase angles are defined in the range $-\pi<\delta\le\pi$. By using a transformation of coordinate system and setting x' and y' as a new axes along the principal axes of the ellipse, the equation (2-6) can be diagonalized as

$$(\frac{E_{x'}}{a})^2+(\frac{E_{y'}}{b})^2=1, \tag{2-7}$$

where a and b are the principal axes of the ellipse, $E_{x'}$ and $E_{y'}$ are the electric field vector components in the principal coordinate system. As demonstrated in Fig. 2-10, if the angle ϕ of transformation of coordinate is between 0 and π, the length of the principal axes are then given by

$$a^2 = A_x{}^2 \cos^2\phi + A_y{}^2 \sin^2\phi + 2A_xA_y \cos\delta\cos\phi\sin\phi \qquad (2\text{-}8)$$

$$b^2 = A_x{}^2 \sin^2\phi + A_y{}^2 \cos^2\phi - 2A_xA_y \cos\delta\cos\phi\sin\phi \qquad (2\text{-}9)$$

The angle ϕ can be determined by A_x, A_y and cosδ as

$$\tan 2\phi = \frac{2A_xA_y}{A_x{}^2 - A_y{}^2}\cos\delta \qquad (2\text{-}10)$$

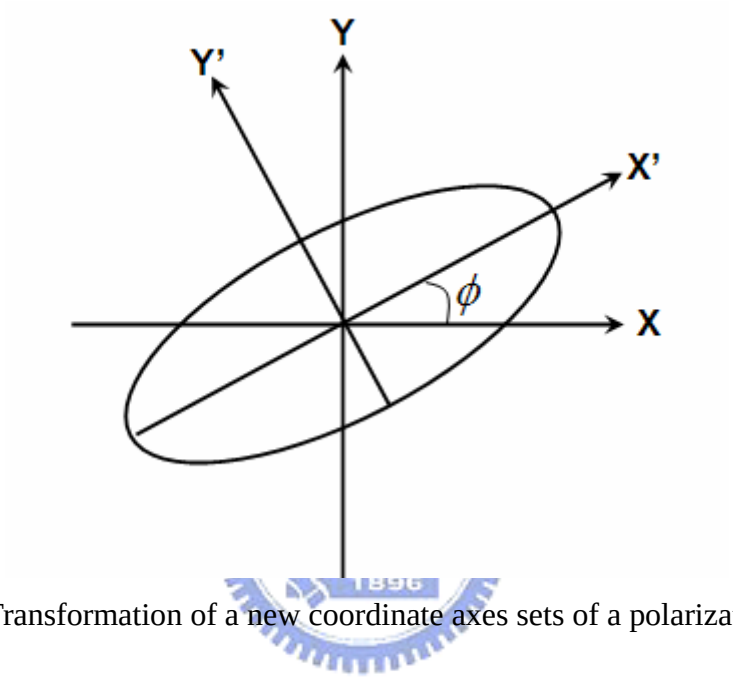

Fig. 2-10. Transformation of a new coordinate axes sets of a polarization ellipse.

The sense of revolution of an elliptical polarization is determined by the sign of sinδ. The end point of the electric vector will resolve in a clockwise direction for sinδ > 0 while in a counterclockwise direction for sinδ < 0. According to Equation (2-6), the ellipse will reduce to a straight line when the phase difference

$$\delta = \delta_y - \delta_x = m\pi \qquad \text{(m=0,1)} \qquad (2\text{-}11)$$

In this case, the light is linearly polarized and the ration of components of the electric field vector is a constant.

$$\frac{E_y}{E_x} = (-1)^m \frac{A_y}{A_x} \qquad (2\text{-}12)$$

According to Equation (2-6), the ellipse will reduce to a circle when the phase

difference

$$\delta = \delta_y - \delta_x = \pm\frac{1}{2}\pi \tag{2-13}$$

and

$$A_x = A_y \tag{2-14}$$

For circular polarization, if the end of the electric field vector is seen to move in a counterclockwise direction by an observer facing the approaching wave, the field is said to possess right-handed polarization. Otherwise, the field is in left-handed polarization. Therefore, when $\delta = -\frac{1}{2}\pi$, the light corresponds to the right-hand circular polarization. In contrast, the light corresponds to the left-hand circular polarization when $\delta = +\frac{1}{2}\pi$.[9]

In order to simplify the polarization rotation in an optical system that consists of several birefringent elements, Jones matrix, which the state of polarization is represented by a 2×2 matrix, is commonly used. When light propagates in a birefringent crystal, such as a phase retardation plate, two egienwave components of light along the slow and fast axes in the crystal, respectively, will propagate with their own phase velocities and polarizations. Because of the difference in phase velocity, one component is retarded with respect to the other, thus, changing the polarization state of light. The phase retardation is given by

$$\Gamma = (n_s - n_f)\frac{\omega d}{c}, \tag{2-15}$$

where d is the thickness of plate and ω is the frequency of the light. For half-wave plate, the phase retardation Γ equals to π. As mentioned in the equation (2-15), the thickness $d = \frac{\lambda}{2}(n_e - n_o)$. We will determine the effect of a half-wave plate on the polarization state of the transmitted light. The azimuthal angle, which is defined as the angle between the plane of polarization and the plane of incidence, of the wave plate is taken as 45° with respect to a vertically polarized incident light. The Jones vector

for the incident light can be written as [10]

$$V = \begin{pmatrix} 0 \\ 1 \end{pmatrix}, \tag{2-16}$$

while for the half-wave plate written as

$$W = \frac{1}{\sqrt{2}}\begin{pmatrix} 1 & -1 \\ 1 & 1 \end{pmatrix}\begin{pmatrix} -i & 0 \\ 0 & i \end{pmatrix}\frac{1}{\sqrt{2}}\begin{pmatrix} 1 & 1 \\ -1 & 1 \end{pmatrix} = \begin{pmatrix} 0 & -i \\ -i & 0 \end{pmatrix} \tag{2-17}$$

The Jones vector for the output light is obtained by multiplying Eqs. (2-16) and (2-17), the result is

$$V' = \begin{pmatrix} -i \\ 0 \end{pmatrix} = -i\begin{pmatrix} 1 \\ 0 \end{pmatrix} \tag{2-18}$$

The output light is horizontally polarized. The effect of the half wave plate is to rotate the polarization by 90°. Therefore, for an arbitrary azimuth angle ψ, the half-wave plate will rotate the polarization by an angle 2ψ. In other words, linearly polarized light remains linearly polarized. In contrast, when the incident light is circularly polarized, the half-wave plate will convert right-hand circularly polarized light into left-hand circularly polarized light.

For quarter-wave plate, the phase retardation Γ equals to π/2. As mentioned in Equation (2-15), the thickness $d = \frac{\lambda}{4}(n_e - n_o)$. Suppose the azimuthal angle of the wave plate is 45° with respect to a vertically polarized incident light. The Jones vector for the quarter-wave plate written as

$$W = \frac{1}{\sqrt{2}}\begin{pmatrix} 1 & -1 \\ 1 & 1 \end{pmatrix}\begin{pmatrix} e^{-i\pi/4} & 0 \\ 0 & e^{i\pi/4} \end{pmatrix}\frac{1}{\sqrt{2}}\begin{pmatrix} 1 & 1 \\ -1 & 1 \end{pmatrix} = \frac{1}{\sqrt{2}}\begin{pmatrix} 1 & -i \\ -i & 1 \end{pmatrix} \tag{2-19}$$

The Jones vector for the output light is obtained by multiplying Eqs. (2-16) and (2-19), the result is

$$V' = \frac{1}{\sqrt{2}}\begin{pmatrix} -i \\ 1 \end{pmatrix} = \frac{-i}{\sqrt{2}}\begin{pmatrix} 1 \\ i \end{pmatrix} \tag{2-20}$$

This is left-hand circularly polarized light. The effect of a 45°-oriented quarter-wave plate is to convert vertically polarized light into left-hand circularly polarized light. In

contrast, for horizontally polarized light, the output light will become right-hand circularly polarized.

2.5 Reflective Polarizer

As we have discussed in **Chapter 1**, the light utilization efficiency of LCD module is only about 8%. The issue of increasing the light utilization efficiency of LC cell that use polarized light is becoming essential. Reflective polarizers that transmit one polarization and recycle the orthogonal polarization is hence developed. The 3M company has developed the reflective linear polarizer, Dual Brightness Enhancement Film (DBEF), which consists of laminated multilayer. Each layer contains an isotropic and a birefringent film. The refractive indices for the ordinary axis in the birefringent film and for the isotropic film are equal. Thus, the stack of layers is isotropic for linearly polarized light in the direction of the ordinary axis. Light which polarized direction is parallel to the ordinary axis can pass.[11] The complimentary light which polarized in the direction of the extraordinary axis is reflected if the periodicity of the stack and wavelength are matched. The reflected polarized light is again reflected by a depolarizing diffuser. And hence light is again treated the same way as the previous incoming light, as shown in Fig. 2-11.

Compared with backlight using conventional polarizers, 60% gain in luminance is obtained. Nevertheless, a stack of alternate isotropic and birefringent films is complex in fabrication. Additional cost and thickness are the targets to be eliminated.

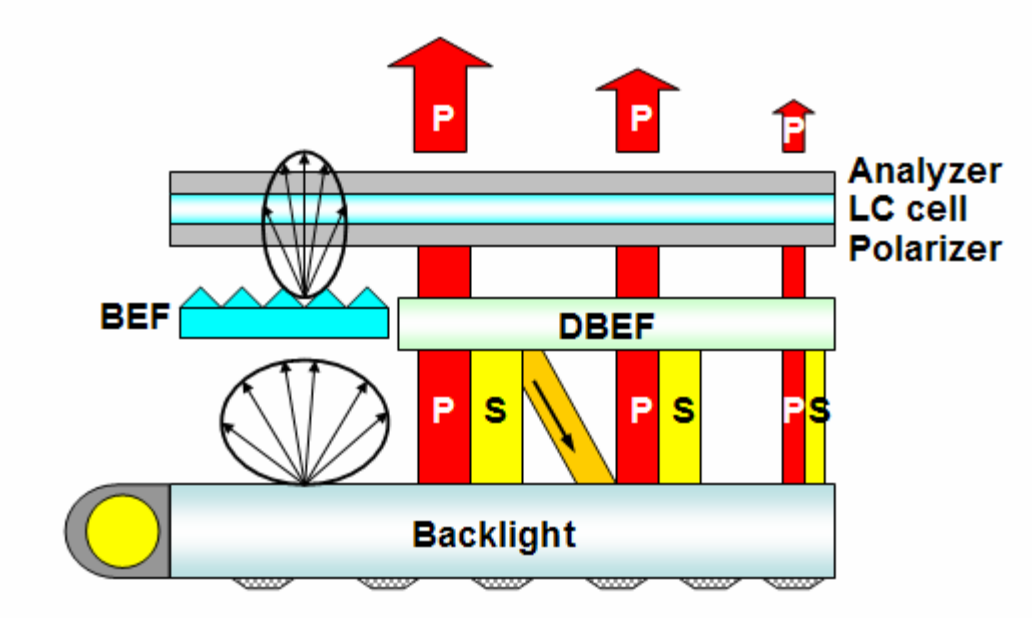

Fig. 2-11. The operation of BEF and DBEF.

Philips introduced another type reflective polarizer, which is composed of a birefringent foil with a helical molecular structure.[12] The helical structure is generated by a planar oriented cholesteric liquid crystal film. The helix only allows light circularly polarized in the opposite sense of the helix to pass. The light circularly polarized in the same sense as the helix is reflected. The central wavelength of the reflected light corresponds to the pitch p of the molecular helix according to $\lambda_0 = \bar{n} \times p$. Here $\bar{n} = (n_e + n_0)/2$ is the average of the extraordinary and the ordinary refractive index, n_e and n_o, respectively. The reflection wavelength can be adjusted by an appropriate selection of the cholesteric material or by a balanced blend of a chiral and nematic LC and can be varied from UV to IR light.

The drawback of this type reflective polarizer is a limited bandwidth Δλ for cholesteric filters. The bandwidth is related to the pitch p of the molecular helix and the birefringence $\Delta n = n_e - n_o$ according to $\Delta\lambda = p \times \Delta n$. In the visible spectrum, the bandwidth is mainly determined by Δn. For colorless organic materials, Δn is limited to vaules below 0.3, thus, resulting in $\Delta\lambda < 100$ nm. In general, Δλ is between 30 and

50 nm which is insufficient for full color displays. The limited bandwidth can be solved by the application of a gradient in the cholesteric pitch. A stack of cholesteric layers with adjacent reflection bands, which would require at least three but ideally more, covers the whole visible spectrum. The range of the cholesteric pitch is chosen such that the smallest pitch reflects blue circularly polarized light and the largest pitch reflects the corresponding red light. In the cholesteric reflective polarizer configuration, the pitch of cholesteric helix increases from 240 nm at one side to 410 nm at the other side of film.

The circularly polarized component in the opposite direction as the helix is transmitted, whereas the reflected component undergoes depolarization by scattering as demonstrated in Fig. 2-12.

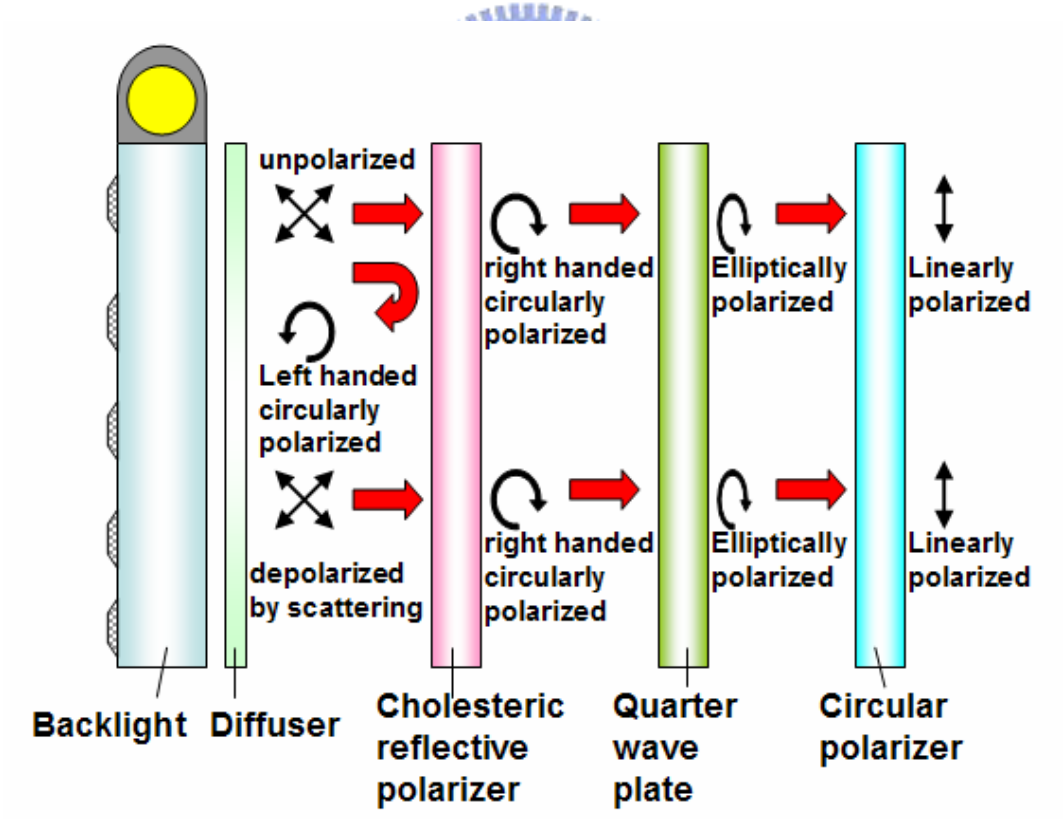

Fig. 2-12. Schematics of the operation of reflective cholesteric reflective polarizers.

This mechanism repeated infinitely. Then, the circular polarized light is

transformed into the linearly polarized light by a λ/4 plate. This solution can enhance the luminous intensity by 42% in comparison with conventional backlight using dichroic polarizers.

2.6 Concerned Issues for LCD Backlight

In the practical design, LCD backlights are limited by inadequate uniformity, brightness, and moiré patterns. In order to meet requirements of human perception, several issues need to be concerned. These concerned issues will be described and discussed in details as follows:

For obtaining a uniform image on LC panel, high uniformity of backlight systems becomes essential to be achieved. Generally, uniformity can be measured by 9-points and 13-points methods for the mobile size and the notebook size of LCDs, respectively.[13] As shown in Fig. 2-13 (a) and (b), 5-points in the central and edge of the backlight are chosen in first. Then, the other points are chosen in the middle of previous 5-points. For the notebook size of LCDs, more points can be selected for more accurate measurement. Next, brightness intensities of these points are measured.

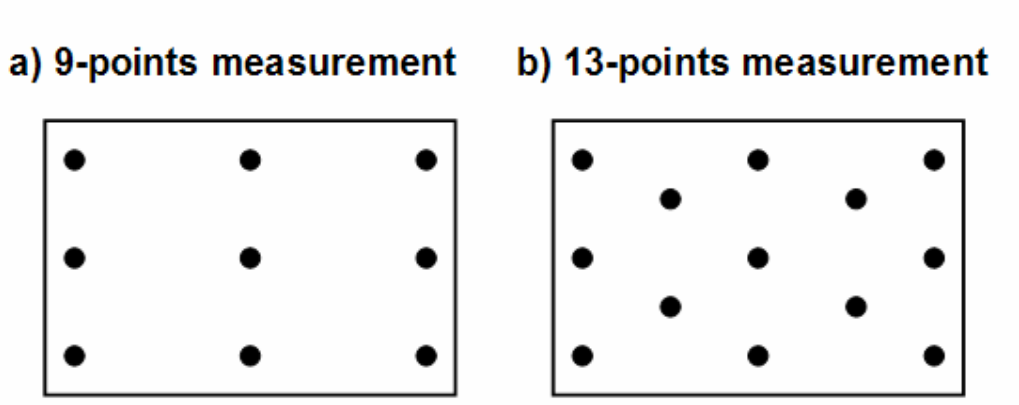

Fig. 2-13. Uniformity of backlights measured by (a) 9-points and (b) 13-points for the mobile size and the notebook size of LCDs, respectively.

And hence uniformity of the backlight is defined as the ratio of the minimum to the maximum brightness intensity, which is expressed in the equation (2-21).

Uniformity=100% ×(the minimum brightness/ the maximum brightness) (2-21)

In general, the requirement of uniformity higher than 80% of LCD backlights needs to be achieved for commercial applications.

Except high uniformity, brightness intensity is also a key factor that influences human perception. Sensation of human eyes for the display is usually determined by brightness and contrast ratio of images. For indoor environment, the requirement of brightness of mobile display is around 50~100 cd/m^2. For outdoor environment, brightness of display needs to be higher. Because the transmission of LC panel is around 6~8%, the requirement of brightness of LCD backlight can be estimated as around 1000 cd/m^2.

Another issue that exists in LCD backlights is moiré pattern effect, which occurs when periodic structures are superposed. Moire pattern usually causes uncomfortable feeling while viewing. The conventional LCD system gives rise to moiré fringes on screen due to the overlapping of LCD pixel structures, grooves of prism sheets, and micro-structures of the lightguide. One way to reduce Moire effects is to defocus the image. Defocusing the image will destroy not only the periodic structures but also the details of the image. When the image is out of focus, the frequency response of the MTF drops in the high frequency region, only low frequencies are unaffected. Another technique is to place a diffuser close to the LC panel. When the diffuser is in contact of the panel, the Morie fringes become inconspicuous.[14] However, these mentioned approaches usually degrade the brightness and contrast ratio of images. Therefore, novel approaches were proposed to suppress moiré patterns by either rotating one periodic structure by a tiny angle or designing adequate ratio of periods of overlapping structures.[15] For example, assume

the period of two stripe structures is *d*, the direction of one stripe structure is parallel to x-axis while the other is inclined an angle θ to x-axis. After overlapping these two stripe structures, moiré patterns can be expressed as Equation (2-24).

$$x=dm_1 \tag{2-22}$$

$$x\cos\theta - y\sin\theta = dm_2 \tag{2-23}$$

$$x(1-\cos\theta) + y\sin\theta = d(m_1-m_2) = dq$$

$$\text{when } \theta \cong 0 \quad \Rightarrow \theta y = dq \quad \Rightarrow \quad y = q\left(\frac{d}{\theta}\right) \tag{2-24}$$

From Equation (2-24), when the inclined angle θ is very small, the period of moiré pattern is proportional to d/θ. And hence the period of moiré pattern increases as the decreasing of θ. For another case, assume the periods of two stripe structures are d and (d+Δ), respectively. After overlapping these two stripe structures, moiré patterns can be expressed as Equation (2-27).

$$x=dm_1 \tag{2-25}$$

$$x=(d+\Delta)m_2 \tag{2-26}$$

$$\frac{x}{d} - \frac{x}{d+\Delta} = m_1 - m_2 = q = \frac{\Delta x}{d(d+\Delta)}$$

$$\text{when } \Delta << d \quad \Rightarrow \quad x = q\frac{d^2}{\Delta} \tag{2-27}$$

From Equation (2-27), when the difference Δ of periods is tiny, the period of moiré pattern is proportional to d^2/Δ. And hence the period of moiré pattern increases as the decreasing of Δ. Because the tiny difference of periods causes the increasing of period of moiré pattern, we usually avoid designing close periods of overlapping periodic structures. Generally, when the ratio of periods of two overlapping structures is larger than 3, the moiré patterns become invisible to human eyes.[15]

2.7 Simulated Procedures

Simulated software becomes urgent in the initial design of backlights for

evaluating its uniformity, brightness, light efficiency and polarization states; thereby achieving requirements of LCD backlights. Therefore, we adopted an optical simulation and analyses program, Advanced Systems Analysis Program (ASAP), which was developed by Breault Research Organization (BRO). Generally analytical procedures in designing LCD backlights can be summarized into four parts, which were described as following.

(i) Source building: Referring to the angular specifications, characteristics of emission of light sources, such as LEDs and CCFLs, can be built in the backlight model. An example is shown in Figs. 2-14 (a), (b), (c) and (d).

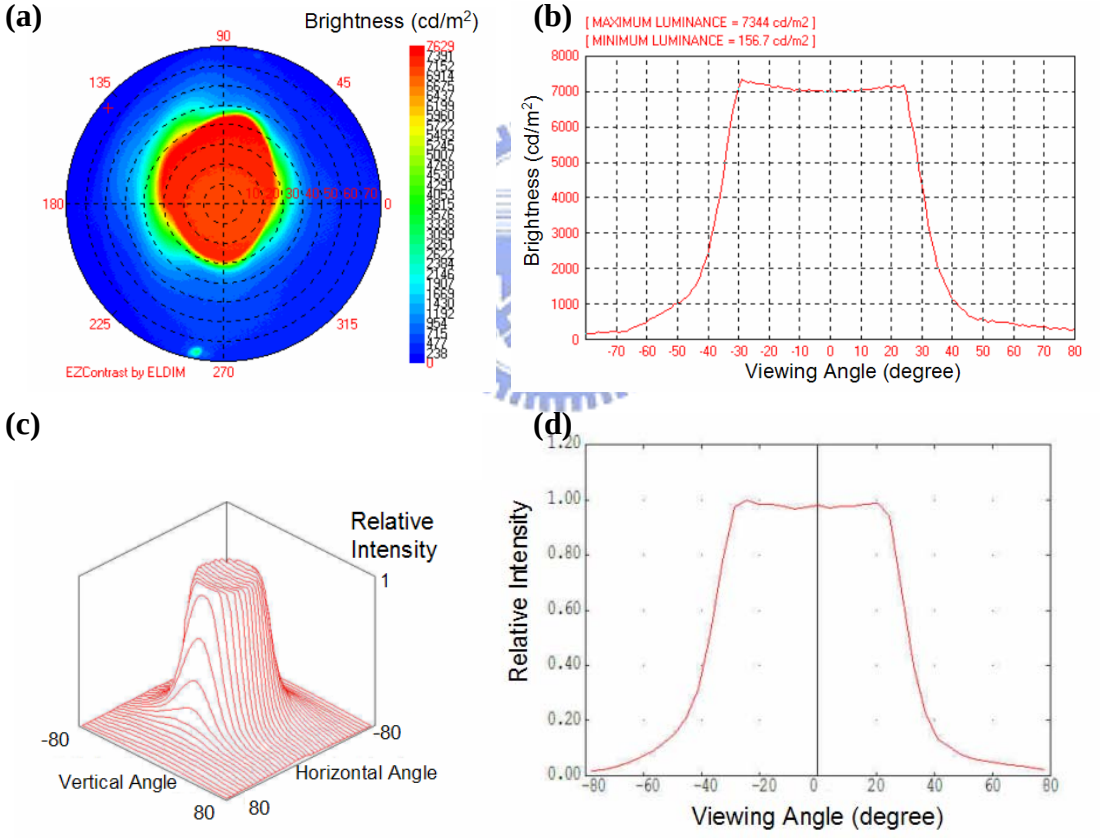

Fig. 2-14. (a) Measured angular profiles, (b) measured angular cross section, (c) simulated angular profiles, and (d) simulated angular cross section of Nichia white light LEDs.

The measured emissive angular profile in polar coordinate of a Nichia white light

LED and its angular cross section are shown in Figs. 2-14 (a) and (b), respectively. In order to build the light source model in ASAP, we simulate the angular cross section shown in Fig. 2-14 (d). The angular cross sections in two orthogonal planes are simulated respectively to build up the 3D angular profiles. In this case, the 3D angular profiles of white light LEDs can be simulated and demonstrated in Fig. 2-14 (c). From the illustrations, the measured angular profiles of Nichia white light LEDs are closely agreed with the simulated emissive angular profiles. Additionally, most of light is distributed within $\pm 35^{\circ}$.

(ii) System modeling: Size, relative positions and surface properties of optical devices are built in the backlight model as shown in Fig. 2-15.

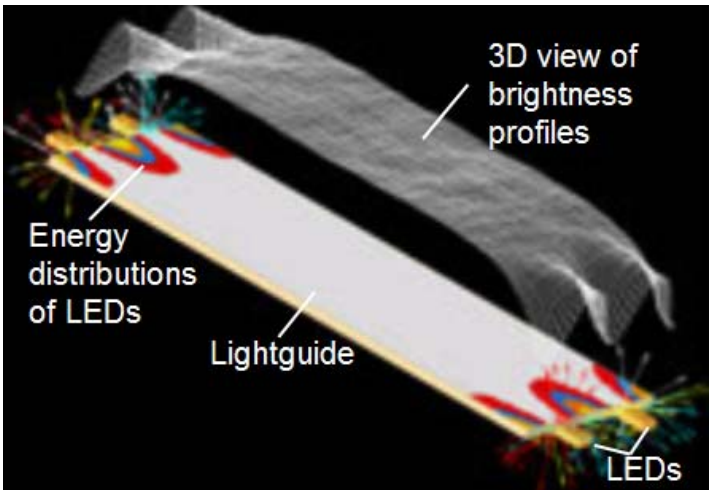

Fig. 2-15. Optical devices of backlights built in the simulation model.

(iii) Ray tracing: Rays from the light sources start tracing in the optical devices of the backlight model, which is shown in Fig. 2-16. The accuracy of simulation usually depends on the number of traced rays. More rays traced ensure the simulated results closer to reality at the expanse of longer simulation time.

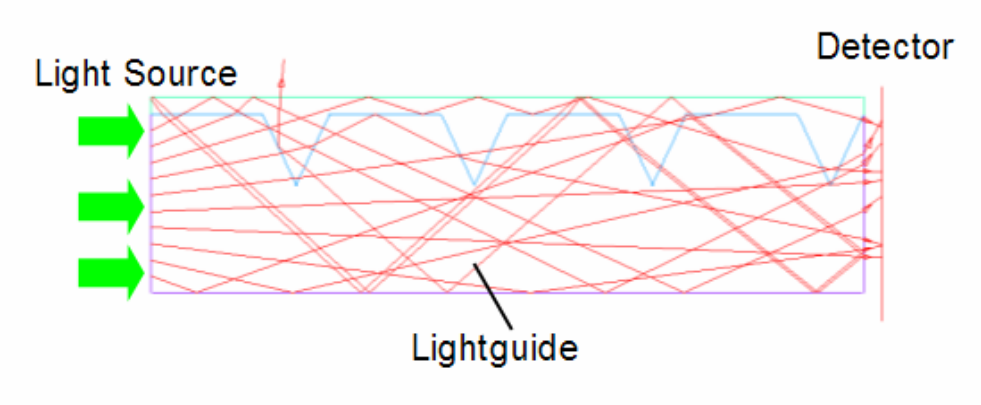

Fig. 2-16. Illustration of Monte Carlo ray tracing in the lightguide.

(iv) Result analyses: After ray tracing, the number, flux, and directional vector of rays on the detector can be recorded and then summarized to obtain brightness and angular profiles as shown in Fig. 2-17. Light efficiency can be also calculated as the ratio of total flux on the detector to the input flux of light source.

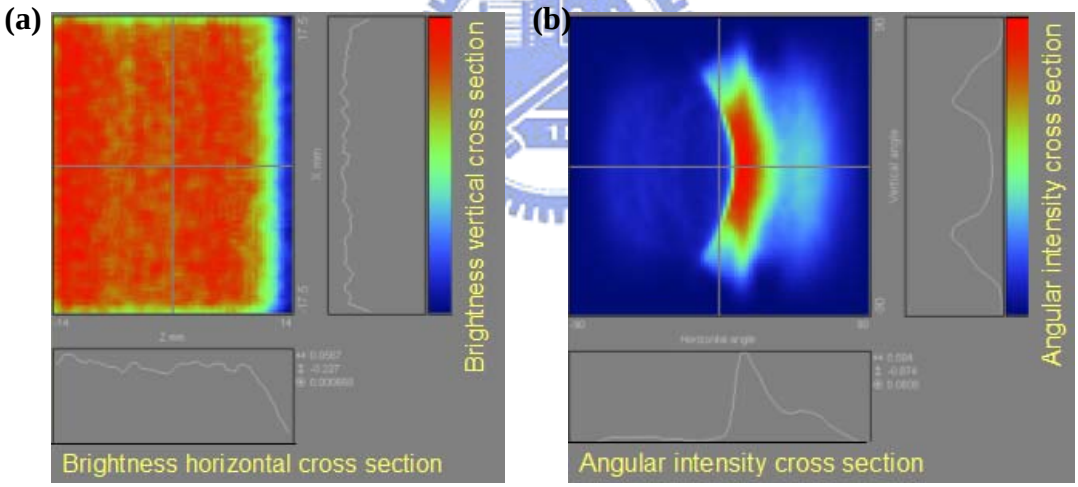

Fig. 2-17. Illustrations of (a) brightness and (b) angular profiles.

Furthermore, in order to achieve adequate uniformity of backlights, array of detectors were built in the backlight model to cover the entire area of backlights at first, which is shown in Fig. 2-18 (a). Brightness profile on each detector corresponds to the number of rays emitted from the respective tiling region of the backlights. Using ray tracing, brightness intensities can be obtained on its respective detector.

Regions with inadequate brightness intensity are then accompanied by tuning the distributed density of micro structures. The distributed density of micro structures can be adjusted by tuning either the size or the pitch of micro structures, which is shown in Fig. 2-18 (b). Next, steps (ii) to (iv) are repeated until nearly equivalent brightness intensities are obtained on the detector array. As a result, adequate uniformity can be achieved. Then, a single detector covering the entire backlight instead of the detector array is used to determine uniformity of backlights by either 9-points or 13-points measurement.

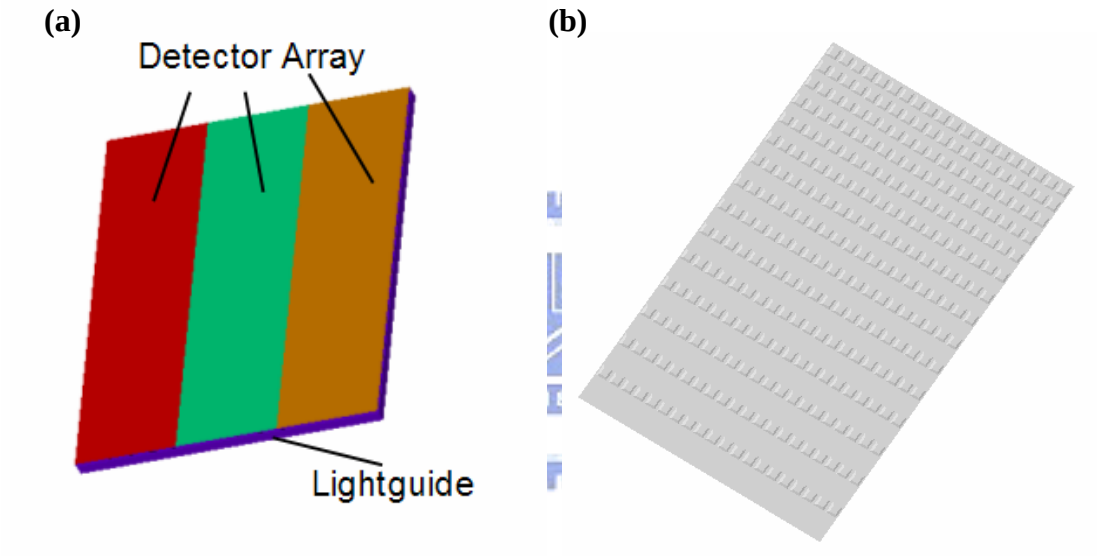

Fig. 2-18. (a) Detector array in the backlight model and (b) gradient distributions of lightguide patterns.

Besides, some research work in this thesis relates to the polarization conversion. ASAP can be also utilized to do the polarized ray tracing. Polarizing devices is simulated as the anisotropic media that has two different indices of refraction dependent on the propagation direction of the optical field within the media. The indices are typically referred to as ordinary and extraordinary. Mueller matrix and the stoke vector is then used to trace the polarization vector in the anisotropic media. As a result, anisotropic foils, phase retarded plates, and polarizers can be modeled. In

order to analyze the polarization state of extracted light from the backlights, a linearly polarizer that can rotate its polarzing axis is hence built in the model between the detector and backlights. Consequently, the polarization state of extracted light can be confirmed.

On the other hand, for accurately calculating the diffraction efficiency of the sub-wavelength grating, the package software, GSOLVER, is introduced in the simulated model. GSOLVER is based on the theory of *Rigorous Coupled Wave Analysis* (RCWA). The parameters of the sub-wavelength grating, such as period, duty cycle, thickness, and materials, can be tuned to achieve the highest diffraction efficiency. As a result, an optimized structure of the grating is determined.

2.8 Summary

Various LCD illumination systems, i.e. LCD backlights, have been briefly introduced and discussed in this chapter. We presented the basic theory and design of LCD backlights. Various micro-optical structures, such as micro reflector, micro-grooves and micro pyramids, were developed and described in the design of LCD backlights. To meet both demands for high uniformity and brightness, several key components of LCD backlights embodiment, such as lightguide, BEF, and diffuser sheet, were introduced.

For further improving the utilization efficiency of LCD backlight, two polarizing devices, DBEF and cholesteric reflective polarizer, were discussed and applied in the display systems to achieve polarization conversion. The basic working principle of various polarizing devices were studied and described. Additionally, the theory of light propagation in birefringent media for polarized light were introduced and ingeniously applied to LCD illumination systems in this thesis work. The mechanism and design rule of these microoptical components in LCD backlights were

presented to facilitate the basis of this thesis. However, in order to exhibit high image quality, several issues, adequate uniformity, high brightness and suppressed moiré patterns, were concerned and discussed in details. Uniformity can be improved by tuning the distribution density of micro structures in gradient. Then, using 9-points and 13-points measurement, uniformity can be determined by the ratio of the minimum to the maximum brightness intensity. To achieve the requirement of commercial applications, uniformity needs to be higher than 80%. One the other hand, moiré pattern phenomenon is caused by the overlapping of periodic structures. There are two approaches to suppress the moiré pattern. One is to rotate one periodic structure by a tiny angle. The other is to design the pitch ratio of periodic structures of larger than 3. In this thesis work, these mentioned fundamental working principles are employed for designing the LCD backlight systems to enhance their efficiency and image performance. Finally, general simulated procedures are concluded and presented for evaluating the functioning of the designed LCD backlights on brightness, uniformity, light efficiency and polarization states.

2.9 References

[1] 葉金娟, 電子月刊第三卷第一期, p. 115 (1997).

[2] K. Kalantar, Society Information Display (SID) Digest, p.764 (1999).

[3] 陳慶偉, 機械工業雜誌六月號, p. 147 (1998).

[4] L. W. Lin, T. K. Shia, and C. J. Chiu, IEEE, p. 1427 (1997).

[5] E. Lueder, *Liquid Crystal Displays*, John Wiley & Sons, p.294 (2000).

[6] K. Kalantar, S. Matsumoto, T. Onishi, K. Takizawa, Society Information Display (SID) Digest, p.1029 (2000).

[7] A. Funamoto, Y. Kawabata, M. Ohira, S. Aoyama, Proceedings of the 11th International Display Workshops (IDW), p.687 (2004)

[8] M. Uekita, Y. Mineo, H. Masaki, Society Information Display (SID) Digest, p.1036 (2000).

[9] A. Yariv, P. Yeh, *Optical Waves in Crystal*, John Wiley & Sons, p.60 (1984).

[10] G. R. Fowles, *Introduction to Modern Optics*, Rinehart and Winston, p. 53 (1975).

[11] 胡文中, 張永昇, 化工資訊十二月號, p.54 (1999).

[12] D. J. Broer, J. A. M. M. Haaren, G. N. Mol, F. Leenhouts, Asia Display, p.735 (1995).

[13] Y. Oki, Society Information Display (SID) Digest, p.157 (1998).

[14] K. W. Chien, C. Y. Tsai, C. M. Chang, H. P. D. Shieh, Society Information Display (SID) Digest, p.938 (2001).

[15] 蔡晴宇, 交大光電所碩士論文, p.18 (1998)